

15597 PIGEONITE BASALTS: EVIDENCE FOR A WET PRIMITIVE LUNAR MANTLE. Xue Su¹ and Youxue Zhang¹, ¹Department of Earth and Environmental Sciences, University of Michigan, Ann Arbor, MI 48109, USA (xuesu@umich.edu)

Introduction: The abundance of H₂O in the primitive lunar mantle is still under debate despite the discoveries of significant water found in various lunar samples including volcanic glass beads and olivine-hosted melt inclusions [1-8] and anorthosites [9, 10]. Melt inclusions provide the most direct evidence for the volatile budget in the pre-eruptive magma although loss must be evaluated. Due to the robustness of H₂O/Ce, F/Nd, Cl/K, and S/Dy ratios to magmatic differentiation processes, these ratios in melt inclusions are used to estimate the volatile abundances (H₂O, F, Cl and S) in the primitive lunar mantle. Even though high H₂O/Ce ratios (~50) have been reported in 74220 olivine-hosted melt inclusions (OH-MIs) [2-5] to suggest a relatively “volatile-rich” primitive lunar mantle, it has been argued that 74220 may just be a local heterogeneity and could not represent the bulk Moon [1] since other studied lunar melt inclusion do not show such high H₂O/Ce ratios [2, 5] and the second highest H₂O/Ce ratio reported is only ~9 from 10020 [2]. The counter argument against a local heterogeneity with 74220 H₂O enrichment includes [2, 5, 11]: (i) other volatiles (F, Cl, etc) are not enriched in OH-MIs in 74220; and (ii) the measured H₂O/Ce ratio in OH-MIs is related to post-eruptive cooling rate of the volcanic material, with higher ratios in more rapidly quenched samples, which is expected due to rapid loss of H₂O from OH-MIs during cooling.

Here we report the H₂O/Ce ratios analyzed from two glassy pyroxene-hosted melt inclusions (PH-MIs), one augite and one pigeonite in 15597 vitrophyric pigeonite basalts. This sample was chosen because it is inferred to have experienced rapid late cooling at 300-500 K/hr [12]. The rapid late-stage cooling is here interpreted to be post-eruptive cooling (the slow early cooling at 3.75 K/hr is interpreted to be pre-eruptive cooling in the magma chamber or the eruption conduit). Such rapid post-eruptive cooling rate is only exceeded by green and orange glass beads, and hence this sample is expected to retain a high H₂O/Ce ratio, only lower than that in 74220. Our preliminary results below confirm this expectation.

Samples and experiments: Lunar sample 15597 is a vitrophyric low-Ti pigeonite basalt (<https://curator.jsc.nasa.gov/lunar/lsc/> and [13]). The pyroxene phenocrysts are typically composed of highly-zoned pigeonite “cores” and augite rims on both exterior and interior of pigeonite “cores” with small melt inclusion near the center (Fig. 1).

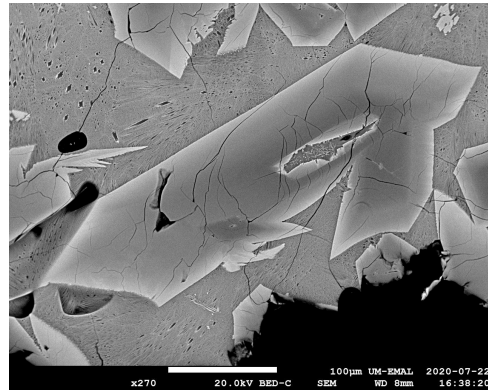


Fig. 1. BSE image of one pyroxene phenocryst with a mostly glassy melt inclusion in the center. The darker part represents pigeonite and the lighter part is the augite “rim”. Note that the augite “rim” is also in the interior of pigeonite, indicating crystallization of augite both inward and outward of pigeonite.

After gently crushing a chunk of 15597 basalt, we hand-picked small basalt pieces with large pyroxene phenocrysts and mostly glassy matrix under optical microscope. Selected pieces were then polished and the ones with measurable glassy melt inclusions were embedded into an indium mount for analyses. Textures of the samples were observed under SEM and major elements were determined using EMPA at the University of Michigan. Two essentially glassy PH-MIs were found, one is about 10 µm by 30 µm, and the other 6 µm by 14 µm. Concentrations of volatiles, refractory trace elements (plus Na, Mg, Al, K, and Ca) and transition metals were measured in three different sessions following this order using SIMS at Caltech. In addition to measuring volatiles in PH-MIs, given the detection of significant amount of water in a nominally anhydrous mineral anorthosite by Hui et al. (2013) [9], we also analyzed volatiles in pyroxenes in 15597 basalts. For melt inclusion analysis, we evaluated whether the second session drilled into pyroxenes. It turns out that for both melt inclusions, pyroxene signals can be identified based on low Na and Al and high Mg and Ca concentrations. The concentrations of refractory elements of the PH-MIs are based on deconvolution of the mixture into melt and pyroxene using many elements. The concentrations of the volatiles are as analyzed.

Results: The larger melt inclusion contains 733 ppm H₂O, and the smaller melt inclusion contains 558 ppm H₂O. The H₂O/Ce ratio based on deconvoluted Ce

concentration is 23 and 22 for the two melt inclusions (without correction, the ratio would be 31 for the larger MI and 127 for the smaller MI). These H_2O concentrations and $\text{H}_2\text{O}/\text{Ce}$ ratios in PH-MIs in 15597 are only lower than those in OH-MIs in 74220, and higher than OH-MIs in all other lunar samples (such as 10020, 74235, 12008, and 12040) as expected from the cooling rates. Fig. 2 shows all available data of $\text{H}_2\text{O}/\text{Ce}$ ratios versus cooling rates in melt inclusions in lunar basalts, including 15597 from this study. Our new data on 15597 demonstrate the positive relation between $\text{H}_2\text{O}/\text{Ce}$ ratio and cooling rate, and support the interpretation that lunar basalts have high pre-eruptive $\text{H}_2\text{O}/\text{Ce}$ ratio of at least 50, and the lower ratios are due to loss of H_2O during post-eruptive cooling.

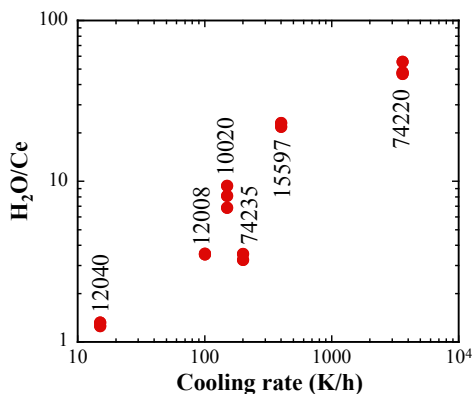


Fig. 2. $\text{H}_2\text{O}/\text{Ce}$ ratio in melt inclusions versus cooling rate of lunar samples. Sample 15597 is from this study. The rest are from [11].

Concentrations of H_2O and F in augite and pigeonite in 15597 are measurable: 14–26 ppm H_2O and 2–4 ppm F. The measured $\text{H}_2\text{O}/\text{Ce}$ ratios in augite (5.6) and pigeonite (53) are used to estimate $\text{H}_2\text{O}/\text{Ce}$ ratio in the melt using partition coefficients in the literature [14–16], leading to $\text{H}_2\text{O}/\text{Ce}$ ratios of 11 to 13 in the equilibrium melt. Considering uncertainties in the partition coefficients, these results are roughly consistent with the melt inclusion data.

The F/Nd ratio in PH-MIs after deconvoluting the pyroxene signal ranges from 4.7 to 7.1, roughly consistent with or slightly higher than those in OH-MIs in other lunar samples (4 ± 1 , [2–7, 11]). Fig. 3 shows the comparison of 15597 glassy PH-MIs with other lunar OH-MIs including 74220, lunar orange and green glass beads, and terrestrial submarine basalts.

Discussions: Ni et al. (2017) [6] showed that there could be noticeable diffusive H loss for OH-MIs of $<50 \mu\text{m}$ diameter, while the two glassy PH-MIs we have found in 15597 so far are smaller than $50 \mu\text{m}$ diameter (one is 10 by $30 \mu\text{m}$ and the other is 6 by 14

μm). Diffusivity of H_2O in pyroxene is not too different from that in olivine [17]. Hence, we are making effort to search for larger glassy melt inclusions in 15597. Larger melt inclusions would be able to preserve H_2O better and we could also circumvent the need to deconvolute melt-pyroxene mixtures. Because H_2O concentration is not deconvoluted, the $\text{H}_2\text{O}/\text{Ce}$ ratios reported here of the two PH-MIs are likely lower than the actual $\text{H}_2\text{O}/\text{Ce}$ ratio in 15597.

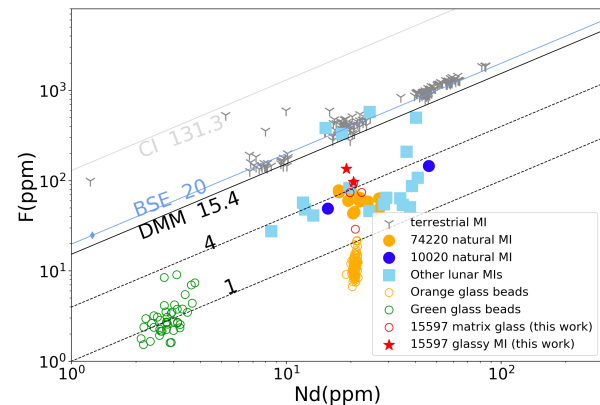


Fig. 3. F versus Nd in 15597 glassy PH-MIs and matrix glass together with previous studies on 74220 MIs [2, 3, 5] and orange glass beads [3], 10020 MIs [2, 5], 15426 green glass beads [3], other reported lunar melt inclusions [5], and terrestrial (MORB&OIB) MIs from GeoRoc and [18–22].

Acknowledgments: We thank NASA CATPEM for providing lunar sample 15597 and Yunbin Guan at Caltech for help with SIMS analyses. This research is supported by NASA grant 80NSSC19K0782.

References: [1] Albarède, F. et al. (2015) *Meteoritics & Planet. Sci.*, 50, 568–577. [2] Chen, Y. et al. (2015) *EPSL*, 427, 37–46. [3] Hauri, E.H. et al. (2015) *EPSL*, 409, 252–264. [4] Hauri, E.H. et al. (2011) *Science*, 333, 213–215. [5] Ni, P. et al. (2019) *GCA*, 249, 17–41. [6] Ni, P. et al. (2017) *EPSL*, 478, 214–224. [7] Saal, A.E. et al. (2008) *Nature*, 454, 192–195. [8] Saal, A.E. et al. (2013) *Science*, 340, 1317–1320. [9] Hui, H. et al. (2013) *Nature Geosci.*, 6, 177–180. [10] Hui, H. et al. (2017) *EPSL*, 473, 14–23. [11] Zhang, Y. (2020) *ACSESC*, 4, 1480–1499. [12] Grove, T.L. and D. Walker (1977) *8th LPSC*, 2, 1501–1520. [13] Weigand, P.W. and L.S. Hollister (1973) *EPSL*, 19, 61–74. [14] Green, T.H. et al. (2000) *Lithos*, 53, 165–187. [15] McKay, G. et al. (1991) *LPSC*, 22, 883. [16] Wade, J.A. et al. (2008) *Geology*, 36, 799–802. [17] Hercule, S. and J. Ingrin (1999) *Am. Min.*, 84, 1577–1587. [18] Danyushevsky, L.V. et al. (2000) *Contrib. to Min. and Petrol.*, 138, 68–83. [19] Dixon, J.E. et al. (2002) *Nature*, 420, 385–389. [20] Michael, P. (1988) *GCA*, 52, 555–566. [21] Michael, P. (1995) *EPSL*, 131, 301–320. [22] Saal, A.E. et al. (2002) *Nature*, 419, 451–455.